August, 2024

Ciudad de Guatemala, Guatemala

Determining the Linear Density of a String via the Catenary Curve

MENDEZ MENDEZ, EDGAR FRANCISCO

Universidad del Valle de Guatemala, Facultad de Ciencias y Humanidades.
Departamento de Física, Física Moderna
Instructor: MSc. Irene Aguilar

ABSTRACT This experiment aimed to determine the linear density (μ) of a string suspended in a catenary curve using theoretical modeling and computational methods. The system of equations derived from the catenary equation and the boundary conditions was solved to match the observed string curve. With boundary points and the total length as inputs, the model produced a predicted curve that closely aligned with the observed data. However, the solution presented a broad range for the linear density, between $0.00026, \frac{kg}{m}$ and $1.742, \frac{kg}{m}$, making precise determination of μ impossible. The actual linear density, confirmed to be $\mu = 0.00802, \frac{kg}{m}$, fell within this range. Sources of error included unmodeled movement along the z-axis and approximations in the string length calculation, leading to a 5.01% error in length determination. The primary challenge was the unknown mass of the string, which limited the accuracy of the model. Despite these challenges, the experiment successfully demonstrated that while this method cannot yield an exact value for linear density, it can provide a viable range. Future work should focus on refining the length approximation technique and using a heavier string to minimize three-dimensional effects.

INDEX TERMS Calculus of variations, Catenary curve, Linear density

I. CONCEPTUAL FRAMEWORK

The catenary curve represents the shape that minimizes potential energy along its length, also known as the equilibrium shape. An ideal catenary is perfectly flexible, non-stretchable, and has uniform mass distribution, though it has no thickness. This minimization of potential energy gives it the characteristic shape [3].

II. OBJECTIVES

- Solve the catenary equation with given boundary conditions.
- Verify the solution against experimental observations.
- Calculate the linear density (μ).
- Develop a program to plot the catenary curve under varying conditions.

III. MATERIALS AND METHODOLOGY

A. MATERIALS

- String
- Kinovea
- Tape measure
- Python

B. METHODOLOGY

A string was taped to a board by Professor Aguilar, and a photo was taken.

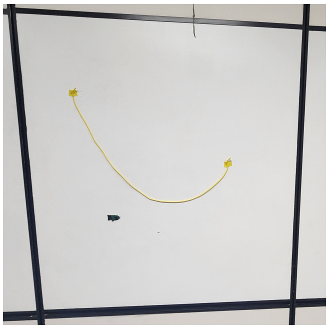

Figure 1: Original setup

Due to camera zoom, distortion is evident. A perspective grid was applied using Kinovea to correct measurements on the distorted plane [2].

The board's dimensions were measured with an error of $\pm 0.005\ m$ and input in centimeters. After corrections, a coordinate grid was aligned with one boundary point.

Coordinates were used to determine distances in x and

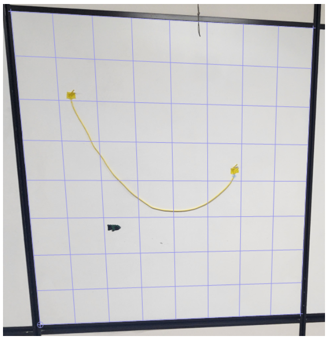

Figure 2: Perspective grid

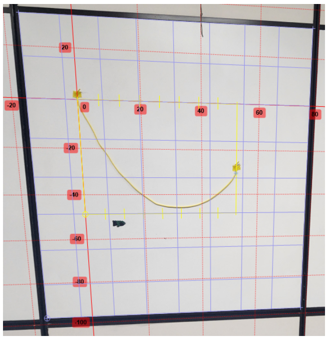

Figure 3: Perspective grid and coordinates

y using Kinovea's measuring tools, which account for grid distortions and have an accuracy of $\pm 0.05\ pixels$ [1].

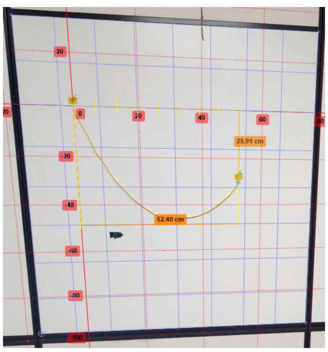

Figure 4: Distances in x(cm) and y(m)

The catenary equation was then solved with the boundary conditions, and the linear density μ was calculated. A program was developed to plot the catenary curve under various conditions.

Additionally, the string length was estimated using a Riemann sum approximation.

C. PRESUPPOSITIONS

To determine the string's linear density, the problem was treated as two-dimensional, disregarding any movement in the z-axis. The string's weight was assumed to be uniformly distributed.

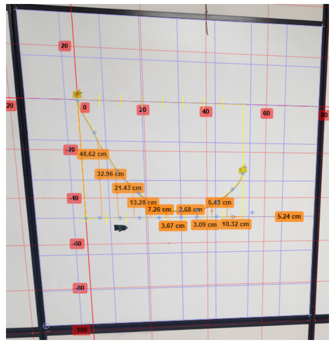

Figure 5: Data for the Riemann sum

IV. EXPRESSIONS AND CONSTANTS

A. EXPRESSIONS

Basic Euler-Lagrange Equation

$$F - y'\left(\frac{\partial F}{\partial y'}\right) = 0 \tag{1}$$

- F is the functional.
- $\left(\frac{\partial F}{\partial y'}\right)$ is the derivative of the functional with respect to y'.
- y' is $\frac{dy}{dx}$.

Potential Energy of the String

$$U = \int_{[x_1,y_1]}^{[x_2,y_2]} \mu g \, d\vec{S} \tag{2}$$

- μ is the linear density.
- g is the gravitational constant.
- $d\vec{S}$ represents the arc length.
- $[x_1, y_1]$, $[x_2, y_2]$ are the boundary points.

Length Constraint

$$L = \int_{x_1}^{x_2} \sqrt{1 + (y')^2}\, dx \tag{3}$$

- L is the string length.
- $\sqrt{1 + (y')^2}$ is the functional.

The Catenary Function

$$F = \int_{x_1}^{x_2} \mu g y \sqrt{1 + (y')^2}\, dx \tag{4}$$

- μ is the linear density.
- g is the gravitational constant.
- y is the string height at any point.

Catenary Euler-Lagrange Equation using Noether's Theorem

$$(\mu g y + \lambda)\left(\sqrt{1 + (y')^2} - \frac{y'}{\sqrt{1 + (y')^2}}\right) = c_1 \tag{5}$$

Solution for the Catenary Equation

$$y = \frac{c_1}{\mu g} \cosh\left[\frac{\mu g}{c_1}(x + c_2)\right] - \frac{\lambda}{\mu g} \tag{6}$$

- c_1 and c_2 are constants.

- λ is the Lagrange multiplier.
- μ is the string's linear density.
- g is the gravitational constant.

Tension of the String at the Lowest Point

$$T_0 = c_1 \mu g \tag{7}$$

- c_1 is the constant that scales the curve according to the tension.
- μ is the linear density.
- g is the gravitational constant.

The Riemann Sum

$$R_s = \frac{\Delta x}{n}(y_1, y_2, \ldots, y_n) \tag{8}$$

- Δx is the horizontal interval.
- y_n is the curve height at each interval.
- $n = 10$ is the number of intervals.

Uncertainty in the Length of the String

$$E_T = \sqrt{\left(\frac{E_x}{\Delta x}\right)^2 + \left(\frac{E_y}{\Delta y}\right)^2} \tag{9}$$

- E_x and E_y are errors in the x and y axes, respectively.
- Δx and Δy are the corresponding changes.

Error Percentage

$$E = \left|\frac{d_t - d_e}{d_t}\right| \cdot 100 \tag{10}$$

- d_t is the theoretic data.
- d_e is the experimental data.

B. CONSTANTS

1) Pixel-to-meter conversion: 1 pixel $= 2.646 \times 10^{-4}\ m$
2) Gravitational constant: $g = 9.811 \pm 0.006$
3) Boundary points:
    - $[x_1, y_1] = [0, 0] \pm 1.32 \times 10^{-5} m$
    - $[x_2, y_2] = [0.5240, -0.2991] \pm 1.32 \times 10^{-5} m$
4) Δx:
    - $0.0524 \pm 1.32 \times 10^{-5} m$
5) String length:
    - $L_s = 0.8813 \pm 0.0209\ m$
6) Length of the board:
    - $L_B = 0.935 \pm 0.005\ m$
7) Height of the board:
    - $H_B = 1.293 \pm 0.005\ m$
8) Actual mass of the string
    - $m_t = 0.0077\ kg$
9) Actual length of the string
    - $L_t = 0.96\ m$

V. RESULTS

$L_t(m)$	$L_{etotal}(m)$	% error
0.96	0.9118	5.011

Table 1: Error in the length

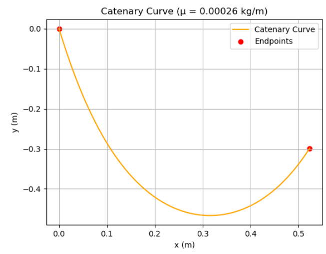

Figure 6: Lower Limit of the Model

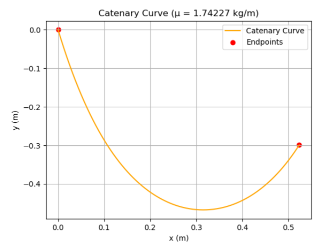

Figure 7: Upper Limit of the Model

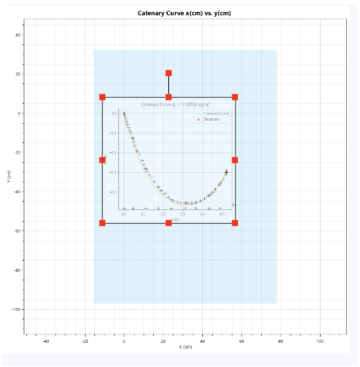

Figure 8: Lower Limit Overlayed with the Adjusted Curve

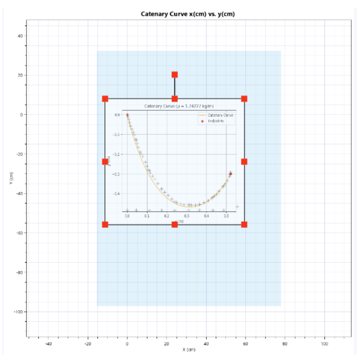

Figure 9: Upper Limit Overlayed with the Adjusted Curve

VI. DISCUSSION

To determine the linear density μ of the string, a system of equations was derived using the catenary equation (6) and the boundary conditions. Given the endpoints:

$$0 = \frac{c_1}{\mu g} \cosh\left[\frac{\mu g}{c_1}(c_2)\right] - \frac{\lambda}{\mu g},$$

and

$$-0.2991 = \frac{c_1}{\mu g} \cosh\left[\frac{\mu g}{c_1}(0.5240 + c_2)\right] - \frac{\lambda}{\mu g},$$

the length constraint (3) was applied:

$$0.8813 = \frac{c_1}{\mu g}\left[\sinh\left(\frac{\mu g}{c_1}(0.5240 + c_2)\right) - \sinh\left(\frac{\mu g}{c_1}(c_2)\right)\right].$$

To fully solve the system, the horizontal tension T_0 at the lowest point was determined using equation (7). This equation arises from the direct relation between c_1 and the tension at the lowest point. The constant c_1 scales the curve according to the tension. Since tension is given by $T = \mu g$, and c_1 serves as a constant of proportionality, equation (7) is derived. Given that neither the tension nor the string's mass was directly measurable, a computational approach was adopted. The program was designed to accept boundary conditions, string length, and a user-specified weight at the lowest point. This allowed for iterative calculations that ultimately aligned a theoretical curve with the observed data. The curve was identical within the linear density interval of $0.00026\frac{kg}{m}$ to $1.742\frac{kg}{m}$. The model would require adjustments in length, tension, and boundary conditions to accommodate a higher linear density.

The overlay of the predicted and observed curves (Figures 8 and 9) demonstrates close alignment. Given such a wide range for the linear density, it would be difficult, if not impossible, to determine the precise linear density based solely on the observations in this experiment. However, as expected, the actual linear density of the string falls within the interval determined by the model.

Potential sources of error in this experiment include unmodeled movement in the z-axis and inaccuracies in calculating the string's length. The Riemann sum used in approximating the string length introduced an error percentage of 5.01%. For future experiments, using the trapezoidal Riemann sum is recommended to obtain a more accurate measurement of the string length.

The greatest challenge in this experiment was the unknown mass of the string, a key factor in calculating μ. Given that the actual linear density is $\mu = 0.00802\,\frac{kg}{m}$, pinpointing this value within the range provided by the model is impossible. On the other hand, if the material of the string had been known, research could have been conducted to estimate its average weight and density, leading to a more precise value for the linear density. Additionally, if the mass were known, the linear density could have been determined directly using the Riemann sum. Another recommendation is to use a slightly heavier string to mitigate any movement in the z-axis.

VII. CONCLUSIONS

- Although the predicted curve closely matches the observed curve, several factors could contribute to deviations, notably errors in the string length measurement and potential three-dimensional effects.
- While the exact linear density could not be determined, the actual linear density lies between $0.00026\frac{kg}{m}$ and $1.742\frac{kg}{m}$ before the model fails.
- This method is not suitable for determining precise values but can provide a range of possible values for the linear density.

References

[1] Joan Charmant. *Uncertainty - men211133@uvg.edu.gt - Universidad del Valle de Guatemala Mail*. (Visited on 08/17/2024).

[2] *Kinovea - Using overlay grids*. URL: https://www.kinovea.org/help/0.8.15/en/103.html (visited on 08/17/2024).

[3] Mark Levi. *Classical Mechanics with Calculus of Variations and Optimal Control*. Vol. 69. The Student Mathematical Library. Providence, Rhode Island: American Mathematical Society, Mar. 7, 2014. ISBN: 978-0-8218-9138-4. DOI: 10.1090/stml/069. URL: http://www.ams.org/stml/069 (visited on 08/16/2024).

VIII. ANNEXES

1) Repository for the determination of the catenary curve: https://github.com/stndred1/The-catenary-utilized

ALL REFERENCE MATERIAL USED.

[1] Jan Awrejcewicz. *Classical Mechanics: Dynamics*. Vol. 29. Advances in Mechanics and Mathematics. New York, NY: Springer New York, 2012. ISBN: 978-1-4614-3739-0 978-1-4614-3740-6. DOI: 10.1007/978-1-4614-3740-6. URL: https://link.springer.com/10.1007/978-1-4614-3740-6 (visited on 08/16/2024).

[2] Gerd Baumann. *Mathematica for theoretical physics*. 2nd ed. New York: Springer, 2005. 2 pp. ISBN: 978-0-387-01674-0.

[3] Joan Charmant. *Uncertainty - men211133@uvg.edu.gt - Universidad del Valle de Guatemala Mail*. (Visited on 08/17/2024).

[4] Michael Cohen. *Classical Mechanics: A Critical Introduction*. Hindawi Publishing Corporation, 2012. ISBN: 978-977-454-109-4.

[5] Walter Dittrich and Martin Reuter. *Classical and Quantum Dynamics: From Classical Paths to Path Integrals*. Cham: Springer International Publishing, 2020. ISBN: 978-3-030-36785-5 978-3-030-36786-2. DOI: 10.1007/978-3-030-36786-2. URL: http://link.springer.

com/10.1007/978-3-030-36786-2 (visited on 08/16/2024).

[6] I. M. Gelfand and S. V. Fomin. *Calculus of Variations*. 1st. Prentic-Hall, Inc., 1963.

[7] Walter Greiner. *Classical Mechanics: Systems of Particles and Hamiltonian Dynamics*. Berlin, Heidelberg: Springer Berlin Heidelberg, 2010. ISBN: 978-3-642-03433-6. DOI: 10.1007/978-3-642-03434-3. URL: https://link.springer.com/10.1007/978-3-642-03434-3 (visited on 08/16/2024).

[8] Jorge V. José and Eugene J. Saletan. *Classical dynamics: a contemporary approach*. Cambridge [England] ; New York: Cambridge University Press, 1998. 670 pp. ISBN: 978-0-521-63176-1.

[9] Hansjörg Kielhöfer. *Calculus of Variations*. Vol. 67. Texts in Applied Mathematics. Cham: Springer International Publishing, 2018. ISBN: 978-3-319-71122-. DOI: 10.1007/978-3-319-71123-2. URL: http://link.springer.com/10.1007/978-3-319-71123-2 (visited on 08/16/2024).

[10] *Kinovea - Using overlay grids*. URL: https://www.kinovea.org/help/0.8.15/en/103.html (visited on 08/17/2024).

[11] Louis Komzsik. *Applied Calculus of Variations for Engineers*. 2nd. CRC Press Taylor and Francis Group, 2008. ISBN: 978-1-4822-5359-7.

[12] Mark Levi. *Classical Mechanics with Calculus of Variations and Optimal Control*. Vol. 69. The Student Mathematical Library. Providence, Rhode Island: American Mathematical Society, Mar. 7, 2014. ISBN: 978-0-8218-9138-4. DOI: 10.1090/stml/069. URL: http://www.ams.org/stml/069 (visited on 08/16/2024).

[13] Mike Mesterton-Gibbons. *A primer on the calculus of variations and optimal control theory*. Student mathematical library v. 50. OCLC: ocn310959874. Providence, R.I: American Mathematical Society, 2009. 252 pp. ISBN: 978-0-8218-4772-5.

[14] Filip Rindler. *Calculus of Variations*. Universitext. Cham: Springer International Publishing, 2018. ISBN: 978-3-319-77636-1. DOI: 10.1007/978-3-319-77637-8. URL: http://link.springer.com/10.1007/978-3-319-77637-8 (visited on 08/16/2024).